Research Project - DMI
3 October 2024

Carlos Becerril
Zhu Jiarui
Om Badagi

Simulation of the Manufacturing Process and Formation Process of the A123 AMP20M1HD-A Pouch Cell.

IMT Nord Europe
École Mines-Télécom
IMT-Université de Lille

RÉPUBLIQUE FRANÇAISE
Liberté
Égalité
Fraternité

I'M TOMORROW

***Abstract*—The purpose of this research project is to simulate the manufacturing process and the formation process of the lithium ion pouch cell A123 AMP20M1HD-A, which is composed of LiFePO4 chemistry. The simulation aims to model the cell behavior during the formation process, focusing on capacity, fading, aging, SEI formation, resistance, state of health (SoH), state of charge (SoC), and temperature, using modeling tools from MATLAB, Simulink, and Simscape. The formation process is a critical step in the battery manufacturing process, where the battery undergoes charge and discharge cycles to stabilize the SEI layer and maximize battery life. The AMP20M1HD-A is a high-performance pouch cell that is used in the electric vehicle due to its long battery life, good thermal conditions, and safety characteristics. The research involves the creation of a battery simulation using Simulink, which includes important factors such as open-circuit potential, temperature sensitivity, and internal resistance. The study explores different formation procedures and their effects on the first dynamic cycle , overall formation efficiency, discharge capacity, and impedance growth. The main findings reveal that the $\mathbf{F}_{86h}$ formation procedure demonstrates the highest initial CE and maintains better capacity retention over 300 cycles compared to shorter formation durations. Analysis of the $\mathbf{F}_{86h}$ protocol exhibits a slower increase in area-specific impedance (ASI), indicating reduced degradation. These results underscore the importance of optimizing the formation process to improve battery performance and longevity, with the $\mathbf{F}_{86h}$ protocol proving to be the most effective in balancing efficiency and long-term stability.**

***Index Terms*—Lithium-ion battery, formation process, A123 AMP20M1HD-A, simulation, MATLAB, Simulink, Battery Simulation, Formation Process, Lithium-Ion, A123 AMP20M1HD-A, Simulink, SEI Growth, SOC (State of Charge), SOH (State of Health), Pouch Cell.**

Simulation of the Manufacturing Process and Formation Process of the A123 AMP20M1HD-A

Carlos Becerril Ceballos, Jiarui Zhu, Om Badagi
IMT Nord Europe
Douai, France
Email: carlos.becerril@etu.imt-nord-europe.fr, jiarui.zhu@etu.imt-nord-europe.fr, om.badagi@etu-etu.imt-nord-europe.fr

CONTENTS

I. Introduction

As one of the core components of new energy vehicles, the battery management system (BMS) collects information from the power battery system, controls, and warns according to the status of the battery system, to ensure that the battery system can be used safely and reliably in new energy vehicles. [1]. As the name suggests, BMS is a system for managing batteries, and its composition includes various control units, monitoring units, information communication units, execution units, etc. The primary task of the BMS is to ensure safety as a premise, so that the battery can play a maximum role in different environmental conditions and operating conditions, and avoid energy waste.Generally speaking, the BMS can be divided into three parts: the controller part, the docking car part, and the monitoring chip part. [1].

A. *Problem Statement*

Challenges in simulating the formation process for lithium-ion batteries. How to simulate SOC,SOH,Cell Balancing and Formation Process models? What data is better to use and how to optimize the large amount of data provided by the type of battery. How to assemble models of different levels of batteries. Objectives: Main goals, such as modeling the SEI layer and simulating pouch cells. Measure the cell and parallel assemble the state of charge, state of health, charge and discharge.

Challenges in simulating the formation process for lithium-ion batteries. How to simulate SOC,SOH,Cell Balancing and Formation Process models. What data is better to use, and how to optimize the large amount of data provided by the type of battery. How to assemble models of different levels of batteries. Objectives: Main goals, such as modeling the SEI layer, simulating pouch cells. Measure the cell and parallel assemble state of charge,state of Health,state of charge and discharge.

II. Lithium-Ion Battery Overview

A. *General Overview*

Lithium-ion batteries (LIBs), widely employed as energy storage devices in contemporary society, offer remarkable advantages including high energy density, cycling performance, and the absence of memory effects. They have become the preferred battery technology in various fields, such as electronic devices, electric vehicles, and renewable energy storage [2]. However, changing societal demands have raised higher performance requirements for LIBs, especially in the electric vehicle industry. To address current concerns about limited driving range, charging speed, and safety, it is imperative to advance battery energy density, improve fast charging capabilities, and improve safety features. Therefore, in-depth investigations of electrode materials, ion-electron-transport mechanisms, and the aging-failure mechanisms of LIBs are of significant importance [3].

B. *Chemistry and Components*

Like other ECCs, a rechargeable LIB is also made of the same components with one or more cells together. Figure 1 illustrates the components of a LIB. The basic structure comprises: • Cathode: positive electrode made up of lithium metal oxide as the cathode on aluminum foil; • Anode: negative electrode made up of carbon as the anode on copper foil; • Electrolyte: lithium salt in organic solvent; • Separator: made up of polyethylene or propylene. During charging, the

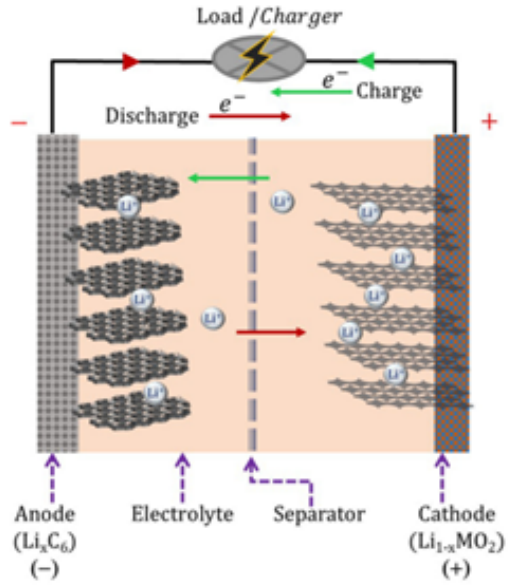

Fig. 1. Components of a LIB

Li ion moves from the cathode to the anode through the electrolyte and electrons through the external circuit. Thus, the external power is used to store energy chemically. During energy utilization, i.e. discharging, the electrons move from the anode to cathode through the external circuit and at the same time the Li ions move back to the cathode via the electrolyte. Thus, LIBs are rechargeable due to the ease with which lithium ions and electrons can be transferred back into negative electrodes. A separator is used to avoid direct contact of the electrodes and only allows the working ion to freely pass through it [4], [5], [6], [7]. The positive electrode, i.e. cathode, is typically made from a chemical compound called layered lithium metal oxide, for example: lithium–cobalt oxide (LiCoO2), and the negative electrode, i.e. anode, is generally made from carbon/graphite compounds [6]. The cathode material that stores lithium ions via electrochemical intercalation must contain suitable lattice sites to store and release ions reversibly, hence material with layered structures may offer stable cyclability and high specific capacity. In addition to this, differential electrochemical potential between the cathode and anode is necessary to obtain a high energy density battery with a given anode. The role of the electrolyte is to act as a medium for the transfer of ions between the two electrodes and to block the electrons [8].

C. *Relevance*

Lithium is the third simplest element, with only three electrons, after hydrogen and helium. In comparison to lead and zinc in conventional batteries, lithium has a substantially higher energy density. It offers the highest specific energy per weight and the highest electrochemical potential. Additionally, molecular mechanisms, such as how lithium can mix with carbon to generate lithium carbonate, are well understood.

There are three key benefits of lithium for batteries:

1) First, it is highly reactive because it readily loses its outermost electron and facilitates current flow via batteries.
2) Second, it is much lighter than other metals used in batteries.
3) Third, it is also a highly reactive element, meaning that a lot of energy can be stored in its atomic bonds, which translates into very high energy density for lithium-ion batteries.

III. Pouch Cell Overview

A. *What is a Pouch Cell?*

Pouch cells look like an aluminum jiffy bag with +ve and -ve terminals protruding from the edge. They need to be

Fig. 2. Pouch Cell

supported mechanically and need a controlled pressure applied to the surface to deliver the power and energy over their lifetime. This is normally achieved by mechanically fixing and supporting the pouches in a well constructed module.

B. *Pouch Cell Pros*

1. pouch cell with tab at each end offers one of the lowest internal resistance cell geometries 2. very high energy density at cell level

C. *Pouch Cell Cons*

1. easy to damage as the cell case offers little protection. 2. maximum thickness of active material stack limited to 15mm. 3. difficult to seal around +ve and -ve tabs and hence limits tab thickness.

D. *Specifications of AMP20M1HD-A*

The AMP20M1HD-A is a lithium iron phosphate ($LiFePO_4$) prismatic pouch cell, manufactured by A123 Systems, primarily used in electric vehicle applications like the Chevrolet Volt. This cell utilizes Nanophosphate technology, which provides high energy density, excellent cycle life, and superior safety characteristics under abuse conditions. Key specifications include a capacity of 19.6 Ah, nominal voltage of 3.3 V, and energy content of 65 Wh. These cells are known for their high power output, which makes them ideal for automotive applications.

IV. Parameters

A. *Battery Main Parameters*

For the parametrization of the Battery (Table-Based) model in Matlab Simulink, parameters from the AMP20M1HD Pouch Cell Datasheet were considered and compared with the parameters of the Matlab block parametrization manager that corresponded to the AMP20M1HD selected part. [9].

1. Vector of State of charge Values: Represents the charge of the cell (%100) considering values from [0 - 1].

Listing 1. Kalman Filter

```
% Kalman Filter
% Vector of state-of-charge values, SOC, (
    Simplified) | (1x7)
SOC_vec = [0, 0.1667, 0.3333, 0.5000, 0.6667,
    0.8333, 1];
```

2. Vector of Temperatures: Represents the temperatures in Kelvin to be analyzed, considering values from [-10° - 35°].

Listing 2. Vector of Temperatures in Kelvin (K)

```
% Vector of temperatures, T (K), (Simplified)
    | Size: 1x3
T_vec = [263.15, 283.15, 308.15]; %
    Corresponding to [-10, 10, 35] (deg C)
```

3. Open Circuit voltage Matrix: Represents the behavior of the voltage (V) while considering the vector of temperatures (K) in a range of values from [2.9322 - 3.3368].

Listing 3. Open-circuit voltage

```
% Open-circuit voltage, V0(SOC,T), (V), (
    Simplified) | (7x3)
V0_mat  = [2.9322, 3.1640, 3.2138;
   3.2449, 3.0131, 3.1632;
   3.2135, 3.2446, 3.0940;
   3.1625, 3.2133, 3.2442;
   3.1749, 3.1617, 3.2131;
   3.2439, 3.2559, 3.1609;
   3.2128, 3.2436, 3.3368];
```

4. Terminal Voltage Operating range: Represents the minimum and maximum operating voltage range [1.8 - 4].

Listing 4. Terminal voltage operating range

```
% Terminal voltage operating range [Min Max] (
    Datasheet Derived) | (1x2)
V_range = [1.8, 4];
```

5. Terminal Resistance Matrix (Matlab Example): Represents the behavior of the terminal resistance (Ohm) of the cell while considering the vector of temperatures (K) in a range of values from [0.0117 - 0.0089].

Listing 5. Terminal resistance

```
% Terminal resistance, R0(SOC,T), (Ohm), (
    Matlab Example) | (7x3)
R0_mat  = [.0117, .0085, .009; .011, .0085,
    .009; .0114, .0087, .0092; .0107, .0082,
    .0088; .0107, .0083, .0091; .0113, .0085,
    .0089; .0116, .0085, .0089];
```

6. Terminal Resistance Matrix (Datasheet Temperature Dependent): Represents the behavior of the temperature dependent terminal resistance obtained from the datasheet specification. However, due to simulation purposes, it was not considered for the model.

Listing 6. Terminal resistance

```
% Terminal resistance, R0(SOC,T), (Ohm), (
    Simplified) | (7x3)
R0_mat  = [0.0800, 0.0489, 0.0192;
   0.0158, 0.0621, 0.0250;
   0.0104, 0.0092, 0.0458;
   0.0101, 0.0053, 0.0046;
   0.0021, 0.0017, 0.0015;
   0.0015, 0.0103, 0.0011;
   0.0012, 0.0014, 0.0019];
```

7. Terminal Resistance Matrix (Datasheet Temperature Independent): Represents the behavior of the temperature independent terminal resistance obtained from the datasheet specification. However, due to simulation purposes, it was not considered for the model.

Listing 7. Terminal resistance

```
% Terminal resistance, R0(SOC), (Ohm), (
    Simplified) | (7x3)
R0_mat  = [0.0035    0.0025    0.0022
   0.0018    0.0017    0.0017
   0.0016    0.0016    0.0016
   0.0016    0.0015    0.0015
   0.0015    0.0015    0.0014
   0.0015    0.0015    0.0015
   0.0015    0.0014    0.0010];
```

Cell Capacity: Represents the Cell Capacity in AH.

Listing 8. Cell capacity

```
% Cell capacity, AH, (A*hr), (Datasheet
    Derived)
AH_min = 19.487; % Minimum
AH = 19.5; % Nominal Ah rating
AH_max = 20; % Maximum
```

B. Model Simplification

Simplification Code: For the parametrization of the Battery (Table-Based) model in Matlab Simulink, parameters from the AMP20M1HD Pouch Cell were simplified as the initial data dimensions were too big to adapt to the desired simulation. Therefore, the simplification allowed the data to reduce its complexity for optimal simulation purposes. The previous parameters shown represent the result of this simplification. In addition, a verification of the simplification was made for comparing that the behavior of the simplified data match the original conditions of the data, by respecting this behavior, such as minimum and maximum values.

1. Vector of State of Charge Values

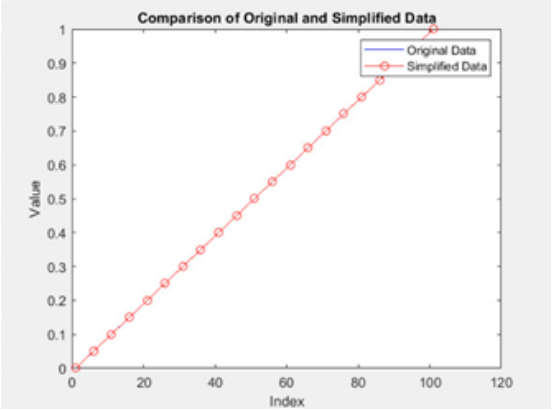

Fig. 3. Vector of State of Charge Values

2. Vector of Temperatures

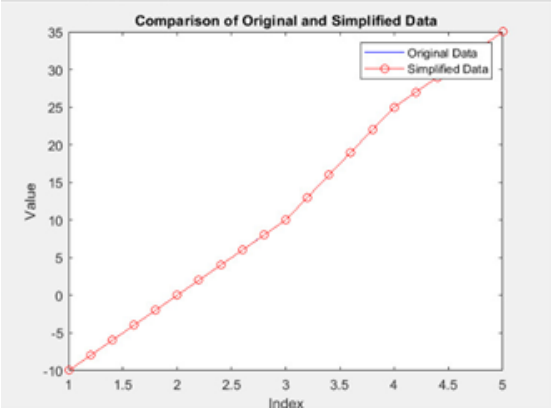

Fig. 4. Vector of temperatures

3. Open Circuit Voltage Matrix

Open circuit voltage matrix. Represents the behavior of the voltage (V) while considering the vector of temperatures (K) in a range of values from [2.9322 - 3.3368].

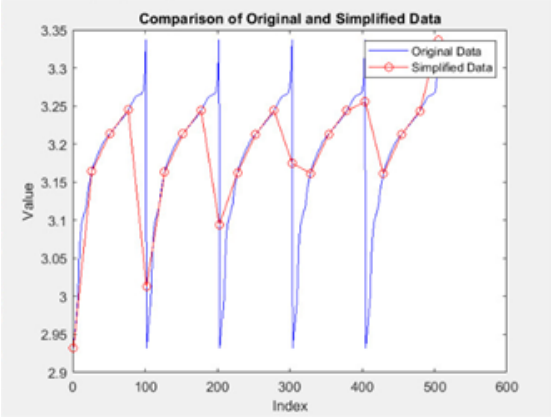

Fig. 5. Open Circuit Voltage Matrix

4. Terminal Resistance Matrix (Matlab Example)

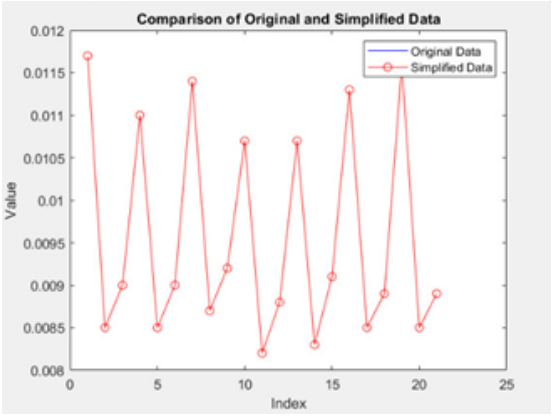

Fig. 6. Terminal Terminal Resistance Matrix (Matlab Example)

5. Terminal Resistance Matrix (Temperature Dependent)

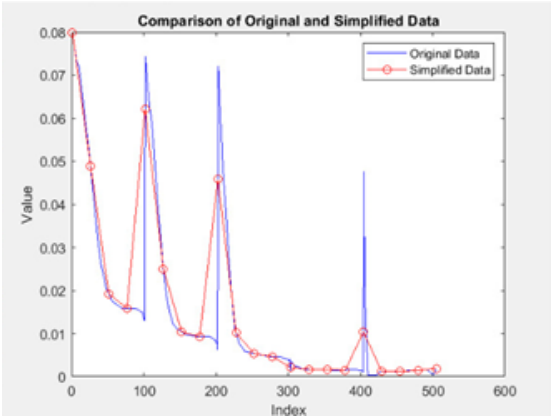

Fig. 7. Terminal Resistance Matrix (Temperature Dependent)

6. Terminal Resistance Matrix (Temperature Independent)

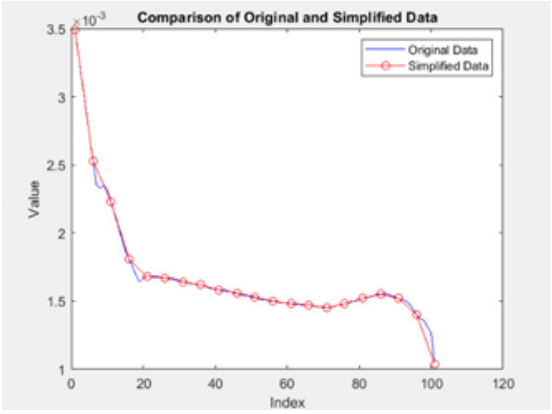

Fig. 8. Terminal Resistance Matrix (Temperature Independent)

C. *Dynamics*

For the system dynamics the behavior of the battery was simulated according to the Matlab examples predefined parameters where the First Polarization Resistance (R1) and the First Time Constant tau were defined in 7 x 3 matrices. [5], [6], [7]

1. First Polarization Resistance

Listing 9. First polarization resistance

```
% First polarization resistance, R1(SOC,T), (
    Ohm), (Simplified) | (7x3)
R1_mat  = [0.0109, 0.0069, 0.0047;
   0.0034, 0.0033, 0.0033;
   0.0028, 0.0029, 0.0024;
   0.0026, 0.0016, 0.0023;
   0.0018, 0.0017, 0.0013;
   0.0012, 0.0013, 0.0010;
   0.0014, 0.0011, 0.0011];
```

2. First Time Constant

Listing 10. First time constant

```
% First time constant, tau(SOC,T), (s), (
    Simplified) | (7x3)
tau1_mat = [20, 31, 109;
   36, 59, 40;
   25, 36, 45;
  105, 29, 77;
   33, 39, 39;
   39, 61, 26;
   67, 29, 33];
```

D. *Fading*

For the parametrization of the Fade the data values were obtained from the Matlab block parametrization manager from the selected part AMP20M1HD Pouch Cell. [1]. In addition, extra parameters were considered, which were obtained from the A123 AMP20M1HD-A Nanophosphate Lithium Ion Rechargeable Cell Datasheet (A123 Systems Inc. 2011.) Which permitted to add more accuracy to the simulation model cell behavior. [2]. For fading purposes the effect of temperature was considered and the behavior of this percentage of change was obtained from the analysis of 4 temperatures [25°, 35°, 45°, 55°] which were considered for better describing our process while taking in consideration the number of cycles from our cell. [[2]. p. 25].

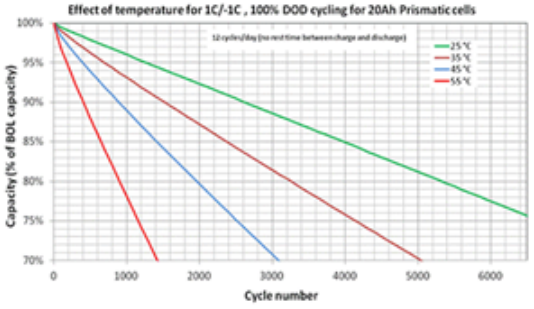

Fig. 9. Effect of Temperature

[[1]. p. 2].

1. Vector of discharge cycle values: This vector represents the range of discharge cycles for the battery in a range from

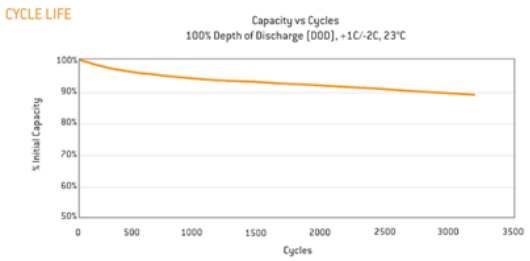

Fig. 10. Cycle Life

[0 - 6436]. However for simulation purposes the number of cycles were divided by 100 in order to simplify the final scopes running simulation in Matlab Simulink.

Listing 11. Vector of discharge cycle values

```
% Vector of discharge cycle values, (N), (Simplified) | (1x6)
N0vec = [0, 1288/100, 2575/100, 3862/100, 5149/100, 6436/100]; % Divided by 100 for simulation purposes
```

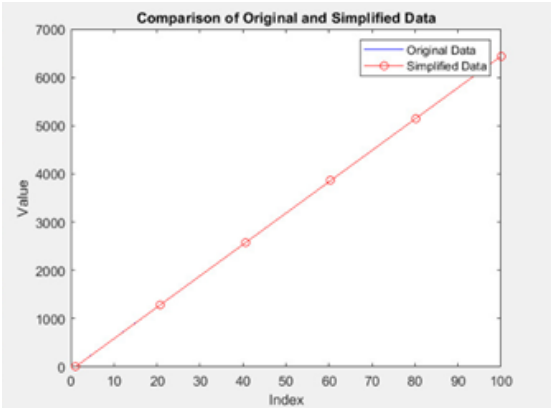

Fig. 11. Vector of discharge cycle values

2. Vector of temperatures for fade data: The vector of temperatures represents the parametrization of the fading effect for the pouch cell, this temperatures are presented in Kelvin and they permit testing the cell at different temperatures and to test its different effects at different temperatures.

Listing 12. Vector of temperatures for fade data

```
% Vector of temperatures for fade data, Tfade (K), (Datasheet Derived) | (1x4)
Tfadevec = [298.15, 308.15, 318.15, 328.15]; % [25, 35, 45, 55] (deg C)
```

3. Percentage change in open-circuit voltage: This matrix represents the percentage of change for the voltage (V) of the cell and its behavior goes in a range from [0 - 2.7693].

Listing 13. Percentage change in open-circuit voltage

```
% Percentage change in open-circuit voltage, dV0(N), (Simplified) | (6x4)
dV0mat = [0, -1.1615, -1.6591, -1.9088;
  -2.0566, -2.1001, -2.1210, -2.1353;
  -2.1506, -2.1651, -2.1800, -2.1948;
  -2.2092, -2.2313, -2.2708, -2.3237;
  -2.3801, -2.4358, -2.4911, -2.5461;
  -2.6010, -2.6558, -2.7123, -2.7693];
```

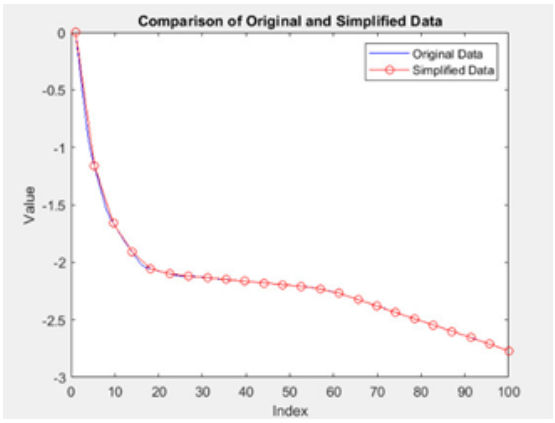

Fig. 12. Percentage change in open-circuit voltage

4. Percentage change in terminal resistance: For the terminal resistance for simulation purposes the value considered for the percentage of change will be 0%. However, according to different documentation after every cycle the terminal resistance is affected, but for simulating purposes considering this percentage is of meaningless impact for the simulation model.

Listing 14. Percentage change in terminal resistance

```
\% Percentage change in terminal resistance, dR0(N), (Simplified) | (6x4)
dR0mat = [0, 0, 0, 0;
    0, 0, 0, 0;
    0, 0, 0, 0;
    0, 0, 0, 0;
    0, 0, 0, 0;
    0, 0, 0, 0];
```

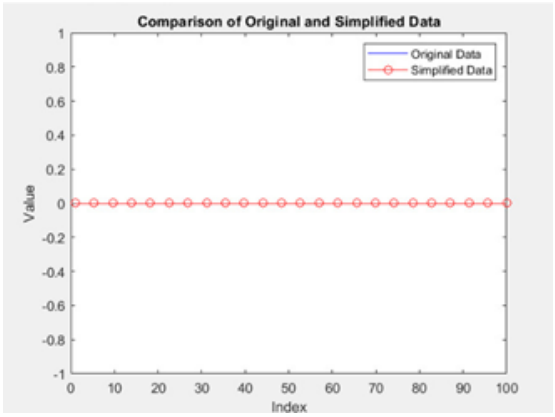

Fig. 13. Percentage change in terminal resistance

5. Percentage change in cell capacity: Considering the percentage of change in cell capacity in fact is of impact for

the model, the following matrix represents a percentage of change of almost 25% for the cell's capacity, starting from value of [0 - 24.73].

Listing 15. Percentage change in cell capacity

```
\% Percentage change in cell capacity, dAH(N),
    (Simplified) | (6x4)
dAHmat = [ 0, -1.2651, -2.3383, -3.4025;
  -4.4758, -5.5605, -6.6402, -7.6515;
  -8.6602, -9.7417, -10.8563, -11.9677;
 -13.0148, -14.0555, -15.0992, -16.1560;
 -17.2235, -18.2975, -19.3641, -20.4263;
 -21.4854, -22.5423, -23.6331, -24.7330];
```

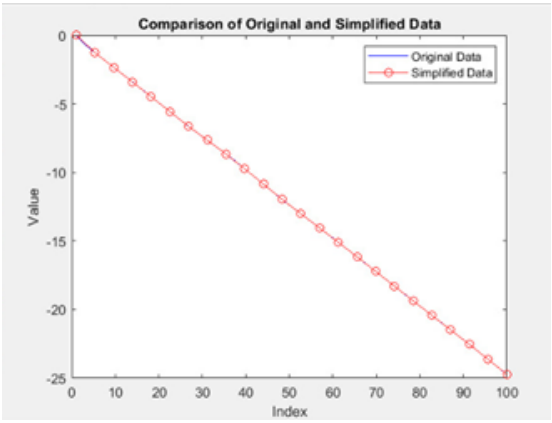

Fig. 14. Percentage change in cell capacity

6. Percentage change in first polarization resistance: As mentioned before and as it was done for the terminal resistance, the value considered for the percentage of change will be 0%.

Listing 16. Percentage change in first polarization resistance

```
% Percentage change in first polarization
    resistance, dR1(N, Tfade)
dR1mat = [0, 0, 0, 0;
     0, 0, 0, 0;
     0, 0, 0, 0;
     0, 0, 0, 0;
     0, 0, 0, 0;
     0, 0, 0, 0];
```

The performance and durability of lithium-ion batteries are significantly influenced by the formation and expansion of the solid electrolyte interphase (SEI) layer. Various aspects of battery operation, including capacity retention, cycling stability, and overall safety, are significantly impacted by the growth of the SEI layer. Here are the key ways in which SEI growth affects battery performance over time: The SEI layer plays a crucial role in safeguarding the anode material from direct contact with the electrolyte, thereby preventing undesired side reactions. An adequately developed SEI layer facilitates the passage of lithium ions while inhibiting electrolyte decomposition at the anode surface. However, an excessively thick or unstable SEI layer can hinder lithium-ion transport, leading to diminished capacity retention over time. An ideal SEI layer

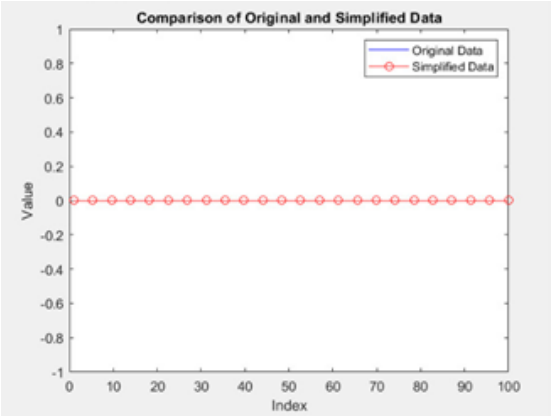

Fig. 15. Percentage change in first polarization resistance

should be thin enough to enable efficient ion transport while remaining stable enough to prevent further decomposition. The stability of the SEI layer has a direct impact on the battery's cycling performance. Continuous formation and dissolution of the SEI layer during charge and discharge cycles can result in changes in its composition and thickness. If the SEI layer is unstable, it can cause increased resistance, resulting in poor cycling stability and capacity degradation. A stable SEI layer helps maintain consistent electrochemical performance, allowing for more cycles before significant capacity loss occurs. SEI Layer: The growth of the SEI layer contributes to the overall impedance of the battery. A thicker or more resistive SEI layer increases the charge transfer resistance, which can slow down the battery's response during high-rate charging and discharging. This increased impedance can lead to reduced power output and efficiency, particularly in applications requiring rapid energy delivery. Lithium Plating: Proper formation of the SEI layer is crucial in preventing lithium plating on the anode when the battery is being charged. If the SEI layer is not formed adequately or is compromised, lithium plating can occur, particularly at low temperatures or high charging rates. This not only reduces the available lithium for intercalation but also presents safety hazards, such as dendrite formation that can cause short circuits. Thermal Stability: The composition and stability of the SEI layer can impact the battery's thermal behavior. A stable SEI layer can help reduce the risks associated with thermal runaway by acting as a barrier against further electrolyte decomposition. On the other hand, an unstable SEI can result in exothermic reactions that raise the risk of overheating and potential failure. Self-Discharge Rates: The SEI layer can also influence the self-discharge rates of lithium-ion batteries. A well-formed SEI layer minimizes the side reactions between the anode and the electrolyte, thus lowering self-discharge. However, if the SEI layer is porous or unstable, it can lead to increased self-discharge, impacting the battery's shelf life and overall efficiency. Influence of Additives: The use of electrolyte additives can significantly impact the growth and properties of the SEI layer. Certain additives can encourage the formation of a more stable and

conductive SEI, enhancing battery performance. However, it is important to carefully consider the choice of additives, as some may result in undesirable side reactions or negatively alter the properties of the SEI. 4.5. Calendar Aging The Calendar Aging parameters for the simulation were obtained from the documentation [1] and [2]. Where principally they were mainly obtained from the capacity loss documentation, where the calendar aging was adjusted in a range of almost a 1000 days. Which also considered the analysis at three different temperatures [25°, 35°, 45°]. [[2] p. 25].

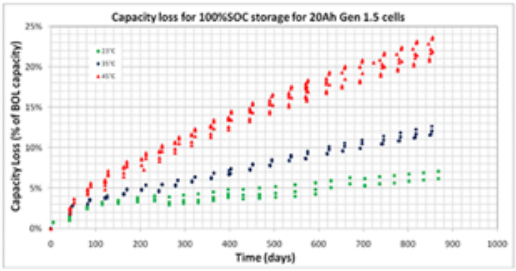

Fig. 16. Capacity Loss due to Calendar Aging

1. Simplified vector of time intervals: The present parameter represents the scale of time for the aging effect of the battery.

Listing 17. Simplified vector of time intervals

```
% Simplified vector of time intervals, (Days),
    (Datasheet Simplified) | (1x3)
storage_dt_age_vec = [0, 500, 1000]; % [0,
    43200000, 86400000] Seconds
```

2. Vector of storage temperatures: The present parameters represent the temperatures considered for the aging effect.

Listing 18. Vector of storage temperatures

```
% Vector of storage temperatures, (K), (
    Datasheet) | (1x3)
storage_T_age_vec = [296.15, 308.15, 318.15];
    % [23, 35, 45] (deg C)
```

3. Vector of sampled temperatures for capacity calendar aging: The parameter corresponds to the simplified vector of storage temperatures.

Listing 19. Vector of sampled temperatures for capacity calendar aging

```
% Vector of sampled temperatures for capacity
    calendar aging, T_ac, (K), (Datasheet) |
    (1x3)
T_age_vec_capacity = storage_T_age_vec;  %
    Same as storage temperatures
```

4.Vector of sampled storage time intervals for capacity calendar aging: The parameter corresponds to the simplified vector of time intervals.

Listing 20. Vector of sampled storage time intervals for capacity calendar aging

```
% Vector of sampled storage time intervals for
    capacity calendar aging, t_ac, (s), (
    Datasheet Simplified) | (1x3)
dt_age_vec_capacity = storage_dt_age_vec;
```

5. Percentage change in capacity due to calendar aging: The parameter corresponds to the simplified vector for the percentage of change in the cell capacity, but by considering the aging effect, based equally at different temperatures.

Listing 21. Percentage change in capacity due to calendar aging

```
% Percentage change in capacity due to
    calendar aging, dAH(t_ac,T_ac), (Datasheet
    Simplified) | (3x3)
dAH_age_mat = [
    0, -2, -5;      % 23 deg C
    0, -3.5, -9;    % 35 deg C
    0, -6, -12      % 45 deg C
];
```

E. Thermal

Thermal Mass: For the thermal model, the thermal mass from the pouch cell was considered based on the documentation studied. [1], [2].

Listing 22. Thermal mass

```
% Thermal mass (J/K)
thermal_mass = 446.4;
```

F. Initial Targets

Initial targets were defined for the current, terminal voltage, initial state of charge, discharge cycles and temperature and during the elaboration of the model, these targets represented initial favorable conditions for the model.

Current

Listing 23. Current

```
\% Current (positive in), (A)
i = 6;
```

Terminal voltage

Listing 24. Terminal voltage

```
% Terminal voltage, (V)
v = 2.9322;
```

State of change: General state of charge for battery cell.

Listing 25. Battery initial SOC

```
% Battery initial SOC
initialSOC = 0.1;
```

Battery 1 initial SOC: State of charge for battery 1 in the parallel assembly

Listing 26. Battery 1 initial SOC

```
% Battery 1 initial SOC
initialSOC1 = 0.1;
```

Battery 2 initial SOC: State of charge for battery 2 in the parallel assembly

Listing 27. Battery 2 initial SOC

```
% Battery 2 initial SOC
initialSOC2 = 0.15;
```

Discharge Cycles: No used battery.

Listing 28. Discharge cycles

```
% Discharge cycles
num_cycles = 0;
```

Temperature: Constant temperature.

Listing 29. Temperature

```
% Temperature, (K)
cell_temperature = 298.15; % 25 deg C
```

G. Nominal Values

Nominal values for the battery cell were respected according to the official documentation obtained. [1], [2]. **Terminal voltage**

Listing 30. Terminal voltage

```
% Terminal voltage, (V)
v_nominal_value = 3.3;
```

State of Charge

Listing 31. Battery final SOC

```
% Battery final SOC
finalSOC = 1;
```

Discharge Cycles

Listing 32. Discharge cycles

```
% Discharge cycles
num_cycles_nominal_value = 6436/100; % Divided
    by 100 for simulation purposes
```

H. Battery Estimation Data

In addition, for upcoming studies for cell design such as the Battery State-of-Charge Estimation, Battery State-of-Health Estimation, Battery Charging and Discharging and Battery Passive Cell parameters from the pouch cell datasheet will be used for simulating the battery cell's behavior model. [1], [2]. **Cell Area:** Parameter obtained from the dimensions of the AMP20M1HD pouch cell.

Listing 33. Cell area

```
% Cell area (m^2)
cell_area = 0.03632; % Length*Width =
    0.160*0.227
```

Heat Transfer Coefficient: Coefficient obtained from the Matlab simulation examples.

Listing 34. Heat transfer coefficient

```
% Heat transfer coefficient (W/(K*m^2))
h_conv = 5;
```

Maximum Cell Voltage: Maximum voltage established in the datasheet.

Listing 35. Maximum cell voltage

```
\% Maximum cell voltage, (Nominal Voltage), (V
    )
vMax = 4;
```

Sample Time: Simulation Defined Time.

Listing 36. Sample time

```
% Sample time (s)
Ts = 1;
```

V. Manufacturing Process

A. Overview of Battery Manufacturing Process

Battery manufacturing, especially for lithium-ion cells, involves several stages, each contributing to the overall performance and reliability of the final product. The process begins with preparing the cell's components, including the electrodes (anode and cathode), electrolyte, and separator. Key steps include:

1) **Mixing:** The active material for the electrodes is prepared by mixing materials like graphite (for the anode) or lithium compounds (for the cathode).
2) **Coating & Drying:** The electrode material is coated onto metal foils and dried. Advances such as dry coating or simultaneous coating of both sides have helped improve efficiency.
3) **Cell Assembly:** The electrodes are wound (for cylindrical or prismatic cells) or stacked (for pouch cells) with the separator in between, followed by electrolyte filling in a dry room to avoid moisture contamination.
4) **Sealing:** The cell is hermetically sealed after filling, and safety features are implemented, like a gas bag for degassing in larger cells.
5) **Formation Process:** The first charging and discharging cycles happen, crucial for forming the Solid Electrolyte Interphase (SEI) layer. This layer stabilizes the cell and influences its self-discharge, performance, and lifespan.
6) **Aging & Testing:** Cells undergo a period of aging to stabilize their properties and are tested for performance metrics like capacity, internal resistance, and leakage before assembly into battery packs. [10]

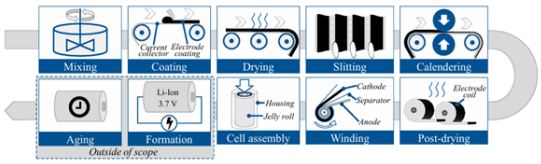

Fig. 17. Process Chain and Individual Process steps used as a basis for the simulation model

VI. Formation Process

The initial charging cycles of lithium-ion batteries involve a crucial process known as the formation of the Solid Electrolyte Interphase (SEI) layer. This layer forms at the boundary between the electrolyte and the electrode and has a significant impact on the performance and lifespan of the battery. By acting as a protective barrier, the SEI layer prevents further reactions between the electrolyte and the anode material, thereby stabilizing the battery chemistry over time. Several factors,

such as the choice of electrolyte, temperature, and the charging protocols used during the formation process, influence the formation of this layer. As part of the formation process, lithium ions from the electrolyte integrate into the anode material, resulting in the reduction of electrolyte components and the creation of the SEI layer. This layer needs to be ionic conductive to enable the passage of lithium ions while simultaneously blocking electrons to prevent additional electrolyte decomposition. A stable SEI is essential to minimize side reactions, which can cause capacity loss and degrade battery performance. As the SEI layer develops, it decreases internal resistance and enhances the overall efficiency of the battery, thus contributing to its cycle life and operational safety. [10].

A. *SEI Layer Formation*

One of the most significant steps in the cell fabrication process is the formation of the solid electrolyte interphase (SEI). Despite irreversibly consuming some amount of lithium from the fresh cathode material, SEI formation is a critical stage in Li-ion cell fabrication. SEI formation enables stable, reproducible cell cycling via controlled reactions at the electrode surface with the electrolyte and its relevant components (salt, additives, solvent). The product of this is a combined substance that passivates the surface layer of the electrode and hinders any further undesirable reaction with the electrolyte. This is particularly important for reactive and porous electrodes such as graphite anodes. According to Wood et al., the SEI layer should be thin, minimally porous, electrochemically inert, electronically resistive, and ionically conductive to Li-ions. Typically, the process of SEI formation has three main stages: During SEI layer formation, it is essential for the electrolyte to maintain constant contact with the electrode surface to ensure uniformity. This is known as wetting and can also be carried out at higher temperatures of 40–60°C to facilitate electrolyte access to the electrode mesopores, which is crucial for proper SEI layer formation. Many companies incorporate multiple wetting stages to meet this requirement, but this can potentially slow down the formation process and increase its cost. The wettability of the electrode is a critical factor for successful SEI formation and is influenced by various factors such as electrode thickness, compression, composition, and cell format. The initial charge/discharge cycles during the formation process are conducted at low and controlled currents to achieve optimal characteristics in terms of SEI composition and thickness, which are essential for minimizing capacity fade in the resulting cell. According to several researchers, the formation process occurs in two successive stages: the first stage involves the creation of an ionically resistive SEI layer at ¿0.25 V vs. Li/Li+, while the second stage involves the conversion of the SEI layer into a highly ionically conductive film at ¡0.25 V vs. Li/Li+. Following the completion of the wetting and formation stages, the aging process begins, which typically lasts 1-2 weeks and includes regular leak current checks. Immediately after formation, leak currents of 20-50 µA cm-2 are expected, but this range gradually decreases to an average of 2-5 µA cm-2 after a few days, and ultimately drops to less than 1 µA cm-2 after a couple of weeks. This process demands significant cycling equipment and floor space, potentially occupying almost a quarter of a production area. [11], [12] .

VII. Battery Parameters in Formation Process

Listing 37. Initial conditions A123 AMP20M1HD-A

```
% Initial conditions A123 AMP20M1HD-A
z0 = {0.05, '1'};                   % Initial SoC,
    z0
Cn = {20, 'A*hr'};                  % Cell capacity
    , Cn
```

Listing 38. Transport A123 AMP20M1HD-A

```
% Transport A123 AMP20M1HD-A
DnRef = {3.9E-14, 'm^2/s'};     % Ref. -ve
    electrode diff. coeff., DnRef
DpRef = {1E-13, 'm^2/s'};       % Ref. +ve
    electrode diff. coeff., DpRef
cn_max = {31507, 'mol/m^3'};    % Maximum -ve
    particle conc., cn_max
cp_max = {22806, 'mol/m^3'};    % Maximum +ve
    particle conc., cp_max
ce0 = {1200, 'mol/m^3'};        % Initial
    electrolyte conc., ce0
tr = {0.2594, '1'};             % Transference
    number, tr
sigma_nRef = {100, 'S/m'};      % Ref. -ve
    electrode conductivity, sigma_nRef
sigma_eRef = {1.2, 'S/m'};      % Ref.
    electrolytic conductivity, sigma_eRef
sigma_pRef = {0.5, 'S/m'};      % Ref. +ve
    electrode conductivity, sigma_pRef
```

Listing 39. OCVs A123 AMP20M1HD-A

```
% OCVs A123 AMP20M1HD-A
sn_max = {0.8, '1'};            % Maximum -ve
    stoichiometry, sn_max
sn_min = {0.01, '1'};           % Minimum -ve
    stoichiometry, sn_min
sp_max = {0.98, '1'};           % Maximum +ve
    stoichiometry, sp_max
sp_min = {0.3, '1'};            % Minimum +ve
    stoichiometry, sp_min
```

Listing 40. Kinetic parameters

```
% Kinetic parameters
knRef = {1E-5, '(A/m^2)/(mol/m^3)^{1.5}'};    %
     Ref. negative electrode reaction rate,
    knRef
kpRef = {5E-5, '(A/m^2)/(mol/m^3)^{1.5}'};    %
     Ref. positive electrode reaction rate,
    kpRef
```

Listing 41. Thermal parameters A123 AMP20M1HD-A

```
% Thermal parameters A123 AMP20M1HD-A
Cp = {110, 'J/K'};              % Heat capacity,
    Cp
T0 = {298, 'K'};                % Initial
    temperature, T0
Tref = {298, 'K'};              % Arrhenius ref.
    temperature, Tref
```

Listing 42. Activation energies A123 AMP20M1HD-A

```
% Activation energies A123 AMP20M1HD-A
Ea_kn = {1, 'kJ/mol'};          % Neg. reaction rate activation energy, Ea_kn
Ea_kp = {1, 'kJ/mol'};          % Pos. reaction rate activation energy, Ea_kp
Ea_Dn = {75, 'kJ/mol'};         % Neg. diff. coeff. activation energy, Ea_Dn
Ea_Dp = {10, 'kJ/mol'};         % Pos. diff. coeff. activation energy, Ea_Dp
Ea_De = {1.2, 'kJ/mol'};        % Elec. diff. coeff. activation energy, Ea_De
Ea_sigman = {80, 'kJ/mol'};     % Neg. cond. activation energy, Ea_sigman
Ea_sigmae = {80, 'kJ/mol'};     % Elec. cond. activation energy, Ea_sigmae
Ea_sigmap = {80, 'kJ/mol'};     % Pos. cond. activation energy, Ea_sigmap
Ea_ksei = {1, 'kJ/mol'};        % SEI reaction rate activation energy, Ea_ksei
Ea_Dsei = {1, 'kJ/mol'};        % SEI diff. coeff. activation energy, Ea_Dsei
Ea_sigmasei = {1, 'kJ/mol'};    % SEI cond. activation energy, Ea_sigmasei
Ea_kLi = {1, 'kJ/mol'};         % Li plating reaction rate activation energy, Ea_kLi
```

Listing 43. Aging Parameters for A123 AMP20M1HD-A

```
% Ageing parameters A123 AMP20M1HD-A
kseiRef = {1E-12, 'm/s'};       % Ref. SEI reaction rate, kseiRef
csei0 = {0, 'mol/m^3'};         % Initial SEI concentration, csei0
Usei = {0, 'V'};                % SEI reaction OCV, Usei
DseiRef = {2E-19, 'm^2/s'};     % Ref. SEI diff. coeff, DseiRef
Msei = {0.162, 'kg/mol'};       % SEI molar weight, Msei
pho_sei = {1690, 'kg/m^3'};     % SEI density, pho_sei
sigma_seiRef = {5E-6, 'S/m'};   % Ref. SEI conductivity, sigma_seiRef
Lf0 = {0, 'um'};                % Initial film thickness, Lf0
kLiRef = {1E-11, 'm/s'};        % Ref. Li plating reaction rate, kLiRef
ULi = {0, 'V'};                 % Li plating reaction OCV, ULi
MLi = {6.94E-3, 'kg/mol'};      % Li molar weight, MLi
pho_Li = {534, 'kg/m^3'};       % Li density, pho_Li
```

Listing 44. Domain geometry for A123 AMP20M1HD-A

```
% Domain geometry for A123 AMP20M1HD-A
Ln = {34E-6, 'm'};          % Negative electrode thickness, Ln
Ls = {25E-6, 'm'};          % Separator thickness, Ls
Lp = {87E-6, 'm'};          % Positive electrode thickness, Lp
eps_n0 = {0.33, '1'};       % Negative electrode initial porosity, eps_n0
eps_s = {0.47, '1'};        % Separator porosity, eps_s
eps_p = {0.335, '1'};       % Positive electrode porosity, eps_p
Area_p = {1027E-4, 'm^2'}; % Positive electrode area, Area_p
Rn = {36.4E-9, 'm'};        % -ve Particle radius, Rn
Rp = {36.4E-9, 'm'};        % +ve Particle radius, Rp
an = {3.84E5, '1/m'};       % -ve surface area density, an
ap = {3.82E5, '1/m'};       % +ve surface area density, ap
```

VIII. SEI Function Model in MATLAB

*A. **Modeling SEI Formation: Detailed explanation of how you modeled the SEI formation process in MATLAB.***

A simplified equation for SEI formation rate dSEI/dt might look like:

$$\frac{d\text{SEI}}{dt} = k \cdot C_{\text{Li}} \cdot e^{-\frac{E_a}{RT}}$$

Where:

k is the reaction rate constant,

C_{Li} is the concentration of lithium ions,

E_a is the activation energy for SEI formation,

R is the gas constant,

T is the temperature in Kelvin.

[13]

Listing 45. SEI Formation Calculation Function

```
function [Lf_bar_new, SEI_capacity_fade, SEI_growth_rate] = calc_SEI_formation(current, SoH_SEI, temp)
    % Constants
    F = 96485;              % Faraday constant [C/mol]
    R = 8.314;              % Universal gas constant [J/K/mol]
    time_step = 10;         % Time step for SEI growth [s]
    k_SEI = 1e-6;           % SEI growth rate constant [m/s]
    A = 0.1;                % Electrode surface area [m^2]
    E_a = 50000;            % Activation energy for SEI formation [J/mol]

    % SEI growth rate equation: dLf/dt = k_SEI * I * exp(-Ea/(R*T))
    SEI_growth_rate = k_SEI * abs(current) * exp(-E_a / (R * temp)); % [m/s]

    % Update SEI film thickness over time
    Lf_bar_new = SoH_SEI + SEI_growth_rate * time_step; % SEI thickness [m]

    % Calculate SEI contribution to capacity fade (assuming proportional relation)
```

```
    SEI_contrib = SEI_growth_rate * time_step;
        % SEI contribution to capacity fade

    % Update total capacity fade due to SEI
        formation
    SEI_capacity_fade = SoH_SEI + SEI_contrib;
end
```

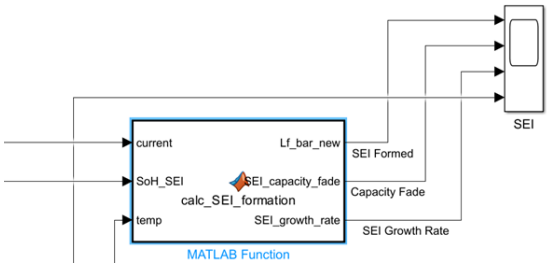

Fig. 18. Modeling SEI Formation

B. *Key Equations and Parameters for SEI Formation*

The SEI growth can be mathematically modeled using diffusion-reaction equations. Typically, the SEI growth rate is expressed as a function of the concentration of lithium ions at the anode surface and the electric potential across the SEI layer. Some models use a combination of Faraday's law and Fick's law to describe the mass transfer of lithium ions and the chemical reactions forming the SEI. A simplified equation for SEI formation rate dSEI/dt might look like:

$$\frac{d\text{SEI}}{dt} = k \cdot C_{\text{Li}} \cdot e^{-\frac{E_a}{RT}}$$

Where:

- k is the reaction rate constant,
- C_{Li} is the concentration of lithium ions,
- E_a is the activation energy for SEI formation,
- R is the gas constant,
- T is the temperature in Kelvin.

[13]

IX. Formation Protocols

A. *Formation Protocols in Manufacturing:*

Formation protocols are critical in the manufacturing and performance optimization of lithium-ion batteries, as they show how the solid electrolyte interphase (SEI) layer is developed on the anode during the initial charging cycles. These protocols can be broadly categorized into single-cycle and multi-cycle strategies, each with its own advantages and challenges. **Single-Cycle Protocols:** Protocols for single-cycle formation are designed to complete SEI formation within a single charge-discharge cycle. This method is appealing as it can significantly shorten the time needed for the formation process, which is crucial for efficient battery manufacturing. However, a key difficulty with single-cycle protocols is the potential risk of lithium plating, which may occur if the charging rate is excessively high or if the potential is not properly regulated. Lithium plating not only diminishes the battery's effective capacity but also poses safety risks, such as dendrite formation that could result in short circuits. Hence, precise optimization of the charging current and voltage limits is vital to ensure adequate formation of the SEI layer without compromising the safety and performance of the battery. **Multi-Cycle Formation:** Formation protocols involving multiple charge-discharge cycles are used in multi-cycle protocols to achieve a gradual and controlled formation of the SEI layer. This approach improves SEI stability and quality by allowing for the gradual buildup of the interphase, which can better accommodate the volume changes associated with lithium-ion intercalation and deintercalation. Multi-cycle protocols also enable adjustments based on observed electrochemical behavior during the formation process to optimize the SEI layer. However, these protocols are time-consuming and may increase production costs, making them less favorable for large-scale manufacturing.

Electrolyte: Several factors, such as the type of electrolyte, electrode materials, and desired battery performance characteristics, influence the design of formation protocols. The choice of electrolyte significantly affects SEI composition and stability, with specific additives promoting the formation of a more robust SEI layer. Additionally, tailored formation strategies may be necessary for electrode materials like silicon or high-voltage cathodes to optimize their performance and address issues such as capacity fading or safety risks.

Temperature: Temperature is a critical parameter during formation, as elevated temperatures can enhance ionic conductivity and expedite SEI formation while also posing the risk of undesirable side reactions compromising the SEI's integrity. Similarly, the current rates applied during formation cycles must be carefully controlled, as excessively high currents can lead to incomplete SEI formation and increased lithium plating, while overly low currents may unnecessarily prolong the formation time.

Assessing and Improving Formation Protocols: Different techniques are used to effectively assess and improve formation protocols. These techniques include non-invasive methods like electrochemical impedance spectroscopy (EIS), which can offer insights into the resistance and stability of the SEI layer, and measurements of charge efficiency that help evaluate the effectiveness of the formation process. Additionally, the use of computational modeling and simulation techniques can assist in predicting the results of various formation strategies, allowing for a more organized approach to protocol development.

B. *Specific Protocols for A123 AMP20M1HD-A*

The Battery A123 AMP20M1HD-A uses the long and traditional form of protocol which is F_86h. [13]

Table 1. Formation protocols used in this study

Formation Protocol	Wetting Conditions	Cycling Conditions	Total Formation Time
F_86h	Tap Charge to 1.5V after vacuum seal, then rest for 6 hours at 30°C.	C/10 CCCV Charge to 4.2 V till Current <C/20, C/10 Discharge to 3.0 V, 4 Cycles. Cycling at 30°C .	86 hours
F_30h	Tap Charge to 1.5V after vacuum seal, then rest for 6 hours at 30°C.	C/2 CCCV Charge to 4.2 V till Current <C/20, C/2 Discharge to 3.0 V, 1 Cycle. C/2 CCCV Charge to 4.2 V till Current <C/20, C/2 Discharge to 3.0 V, 1 Cycle. Cycling at 30°C.	30 hours
F_26h	Tap Charge to 1.5V after vacuum seal, then rest for 6 hours at 30°C.	C/10 CCCV Charge to 4.2 V till Current <C/20, C/10 Discharge to 3.0 V, 1 Cycle. Cycling at 30°C.	26 hours
F_10h	Tap Charge to 1.5V after vacuum seal, then rest for 6 hours at 30°C.	C/2 CCCV Charge to 4.2 V till Current <C/20, C/2 Discharge to 3.0 V, 1 Cycle. Cycling at 30°C.	10 hours
F_10h@40	Tap Charge to 1.5V after vacuum seal, then rest for 6 hours at 40°C.	C/2 CCCV Charge to 4.2 V till Current <C/20, C/2 Discharge to 3.0 V, 1 Cycle. Cycling at 30°C.	10 hours

Fig. 19. *
Specific Protocols for A123 AMP20M1HD-A

C. *Results for Formation Process of A123 AMP20M1HD-A*

Model Used to Simulate the formation process – Charge and Discharge

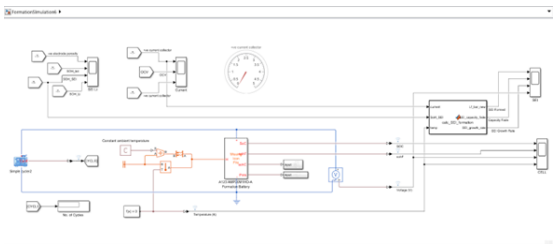

Fig. 20. *
A123 - Formation Process Model

A123 - Formation Protocol F_86h:

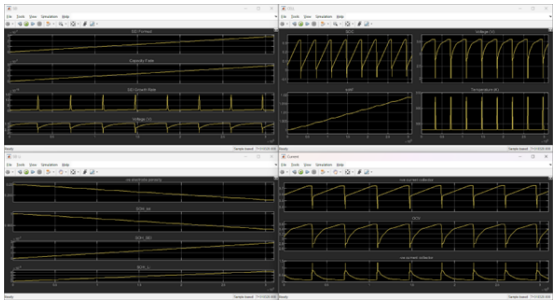

Fig. 21. *
A123 - Formation Protocol F_86h

A123 - Formation Protocol F_30h:
A123 - Formation Protocol F_26h:
A123 - Formation Protocol F_10h:
Li-ion Battery behavior for different Protocols:

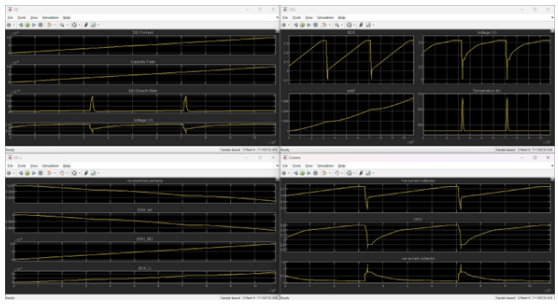

Fig. 22. *
A123 - Formation Protocol F_30h

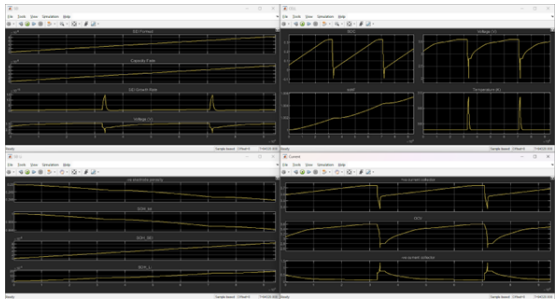

Fig. 23. *
A123 - Formation Protocol F_26h

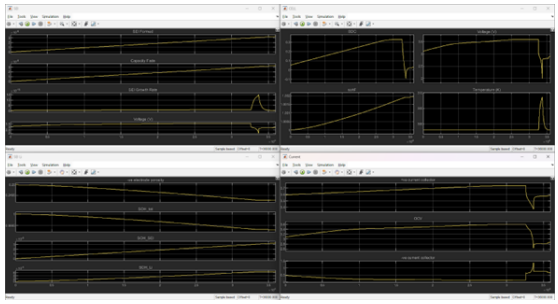

Fig. 24. *
A123 - Formation Protocol F_10h

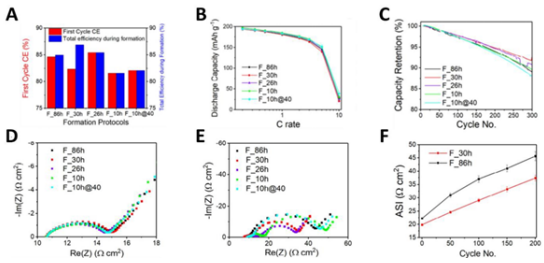

Fig. 25. *
Comparative analysis of various formation protocols

This image presents a comparative analysis of various formation protocols (F_86h, F_30h, F_26h, F_10h, and F_10h@40) for lithium-ion batteries, evaluating their impact on first cycle Coulombic efficiency (CE), total efficiency during formation, discharge capacity, capacity retention, and impedance characteristics.The F_86h protocol shows a slower area-specific impedance growth which indicates better long-term performance compared to protocols. The manufacturing industry uses the F_86 , F_30 protocols to form the battery efficiently and have a long-term battery life. The results of A123 AMP20M1HA-A partially align to the F_86h protocol and behave the same as the other Li-ion Battery.

X. State of Charge (SOC) and State of Health (SOH) Analysis

Battery State-of-Health Estimation Parameters: For properly calculating the state of health the state of charge will be defined by estimating it with the Kalman filter. The following parameters describe the functioning of the estimator which will allow us to properly calculate the state of health of the battery cell.

Listing 46. Kalman Filter

```
%% Kalman Filter
% SOC Estimator (Adaptive Kalman Filter)
Q    = [1e-4 0 0;0 1e-4 0;0 0 1e-4]; % Covariance of the process noise, Q
R    = 0.05; % Covariance of the measurement noise, R
P0   = [1e-5 0 0; 0 1 0; 0 0 1e-5]; % Initial state error covariance, P0
SOC0 = initialSOC; % Estimator initial SOC
R00  = 0.008; % Estimator initial R0
```

A. *Test the model*

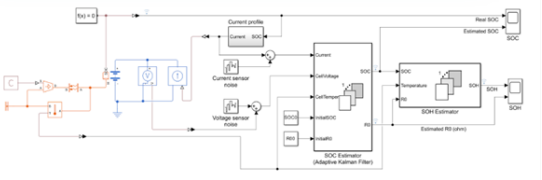

Fig. 26. State of Charge and State of Health Model

This model represents an advanced battery management system (BMS) with **SOC** (State of Charge) and **SOH** (State of Health) estimations using an Adaptive **Kalman Filter**.

Key Components

- **Battery Model:** This part simulates the battery's behavior (A123 AMP20M1HD), including voltage, current, and internal dynamics.
- **SOC Estimator (Adaptive Kalman Filter):** Estimates the battery's SOC using inputs like **current**, **cell voltage**, **temperature**, **initial SOC**, and **R0** (internal resistance). It adapts to changes over time, refining the accuracy of SOC predictions.
- **SOH Estimator:** Uses the SOC, temperature, and internal resistance (**R0**) to estimate the SOH of the battery. SOH reflects the battery's ability to hold charge and maintain performance.
- **Noise Sensor:** Represents inaccuracies in voltage and current measurements due to real-world sensor errors.
- **Flow:** Current, voltage, and temperature are fed into the estimators. SOC is estimated first, which is then used in the **SOH** estimator alongside **R0** to calculate the health of the battery.
- **Real SOC vs. Estimated SOC:** The real SOC and estimated SOC are compared to validate the accuracy of the Kalman filter.

This model is designed to monitor both the charge level and health of the battery, ensuring optimal performance and predicting maintenance needs.

B. *State of Charge (SOC) and State of Health (SOH) Model Results*

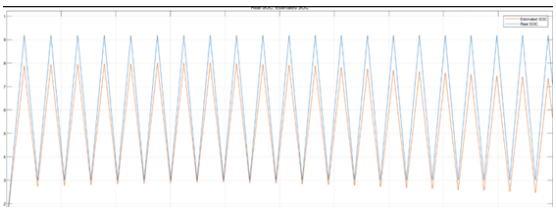

Fig. 27. State of Charge Result

This graph compares the **Real SOC** (blue line) and the **Estimated SOC** (orange line) over time. Real SOC represents the actual state of charge of the battery, while Estimated SOC is the SOC calculated by the model (likely through the Adaptive Kalman Filter). The lines follow a similar trend, with periodic charging and discharging cycles, indicated by the triangular waveform pattern. There is a small offset between the two, where the Estimated SOC slightly underestimates the real SOC during discharge and overestimates it during charging. This discrepancy shows the error in estimation but remains relatively small, meaning the Kalman filter is performing well.

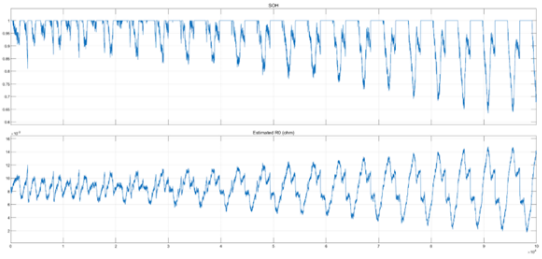

Fig. 28. State of Health Result and R0 Result

SOH (State of Health) Plot (Top) This shows the battery's health over time, where the SOH starts near 1, indicating full health, but decreases to around 0.6 during some intervals. The

sharp drops and recoveries indicate the battery undergoing cycles of stress or load. The SOH fluctuates, showing degradation and recovery patterns, likely due to charging/discharging cycles. **Estimated R0 (Internal Resistance) Plot (Bottom):** The R_0 (ohms) represents the estimated internal resistance of the battery. The resistance fluctuates between 6×10^{-3} ohms and 16×10^{-3} ohms. Higher internal resistance can indicate the battery is aging or being stressed. The two plots together demonstrate that as internal resistance increases, the SOH tends to decrease, reflecting the battery's degradation over time and us

XI. Charge & Discharge

Battery Charge and Discharge: For the charge and discharge estimator the following parameters were selected according to the matlab examples.

Listing 47. Charge & Discharge

```
%% Charging/Discharging Parameters %%
Kp   = 100; % Proportional gain CV controller
Ki   = 10;  % Integral gain CV controller
Kaw  = 1;   % Antiwindup gain CV controller
```

A. *Test the model*

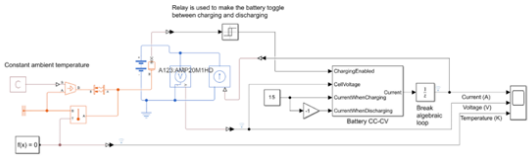

Fig. 29. Charge & Discharge Model

This diagram represents the modeling of a battery system with an A123 AMP20M1HD cell, focusing on the estimation of the State of Charge (SOC) using a Kalman filter.

Key Components

- **Battery model (AMP20M1HD):** This represents the battery cell, outputting current and voltage for further processing.
- **Current/Voltage sensors:** Measure the current and voltage, with added sensor noise to account for real-world inaccuracies.
- **Kalman Filter (SOC Estimator):** Takes current, voltage, cell temperature, and initial SOC values to estimate the SOC, comparing it to the real SOC.
- **Noise blocks:** Add noise to simulate real sensor inaccuracies.
- **SOC feedback loop:** Uses estimated SOC for further analysis.

Key Inputs

- **Current:** The current flowing through the battery.
- **CellVoltage:** The battery's voltage.
- **CellTemper:** The temperature of the cell, which impacts performance.
- **InitialSOC:** The starting SOC of the battery.

The Kalman filter dynamically updates the estimated SOC by processing these inputs and continuously refining the prediction based on measurement errors. This process helps reduce uncertainties and gives a more accurate SOC estimate.

B. *Charge & Discharge Model Results*

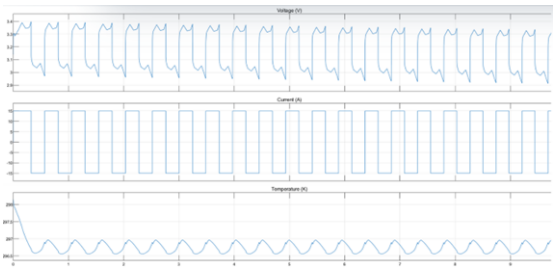

Fig. 30. Charge & Discharge Result

This graph presents the voltage, current, and temperature profiles of a battery system, for the AMP20M1HD-A battery: Voltage (Top Plot): The voltage fluctuates between 2.9V and 3.4V, with a clear charging and discharging pattern. The sharp drops indicate discharge events, while the rising sections correspond to charging periods. Current (Middle Plot): The current alternates between positive and negative values, indicating charging (+15A) and discharging (-15A) cycles, creating a square wave pattern. Temperature (Bottom Plot): The temperature oscillates slightly between 296.5K and 298 K (23.35°C to 24.85°C), showing small increases during charging/discharging cycles.

XII. Balancing

Battery Passive Cell: In addition to increasing the performance of the system, the analysis of the battery balance model will be useful for obtaining a stable model and a better approach for simulating battery assemblies. The threshold parameter used was obtained from the Matlab example.

Listing 48. Balancing

```
%% Balancing Parameters %%
BalThreshold = 0.005;    % Threshold for cell
    balancing (V)
```

A. *Test the model*

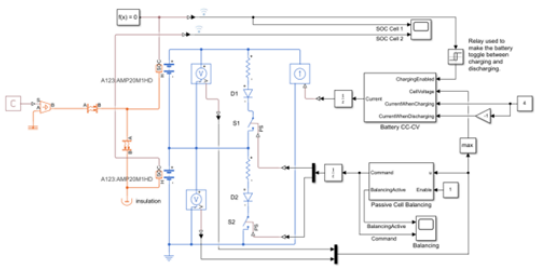

Fig. 31. Balancing Model

This diagram represents a **battery management system** (BMS) with components to control and balance battery cells.
Key Components:

- **A123: AMP20M1HD cells:** Two battery cells monitored and controlled.
- **Relay Control:** Toggles between charge and discharge modes.
- **Current and Voltage Sensors:** Measure the current and voltage across cells.
- **Battery CC-CV (Constant Current - Constant Voltage):** Manages the charging and discharging process using current and voltage feedback.
- **Passive Cell Balancing:** Equalizes the voltage between cells to ensure uniform performance.
- **Insulation:** Isolates components to avoid electrical shorts or interference.

Each part helps to ensure safe, efficient, and balanced charging and discharging.

B. *Balancing Model Results*

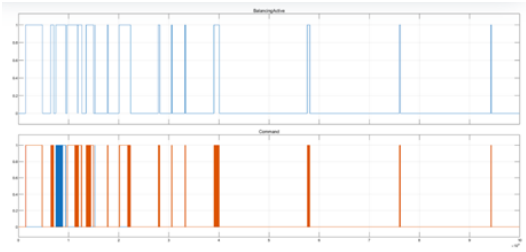

Fig. 32. Balancing Result

Balancing Active (Top Plot): The plot shows a binary state (0 or 1), where "1" indicates that the balancing process is active and "0" means it is inactive. The activity happens intermittently, probably on the basis of specific conditions, such as when the voltage difference between cells exceeds a threshold.
Command (Bottom Plot): This plot also shows binary states, where the command to activate balancing is issued. Rapid shifts between 0 and 1 indicate frequent balancing commands that adjust cell voltages.

This graph shows how the balancing algorithm dynamically manages the cell voltages to make sure they remain balanced over time, toggling based on system conditions.

XIII. Pouch Cell Simulation

A. *Test the model*

This diagram illustrates a simulation model with a **battery management system** (BMS) with a focus on **SOC** (State of Charge) and **SOH** (State of Health) estimation using an Adaptive Kalman Filter.

Key Components

- **A123: AMP20M1HD:** Battery cell model used.
- **Relay:** Toggles between charging and discharging.
- **Battery CC-CV:** Manages constant current and constant voltage for charging.

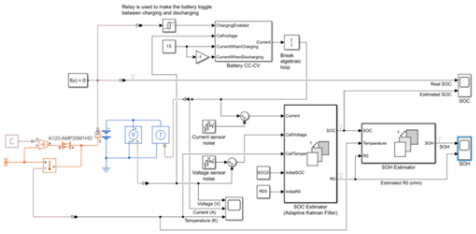

Fig. 33. Pouch Cell Integrated Simulation

- **Current and Voltage Sensor Noise:** Adds realistic measurement noise.
- **SOC Estimator (Kalman Filter):** Estimates battery SOC using inputs such as current, voltage, temperature, and initial conditions.
- **SOH Estimator:** Uses SOC, temperature, and internal resistance (R0) to estimate SOH.

The feedback loops ensure that the SOC and SOH are constantly updated, ensuring efficient management and health tracking of the battery system.

B. *Pouch Cell Simulation Results*

State Of Charge

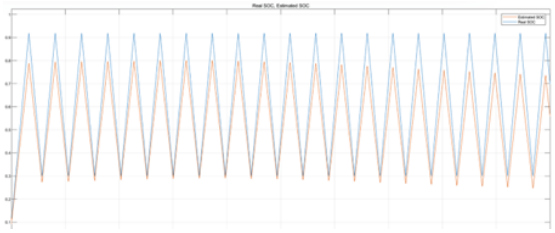

Fig. 34. State of Charge

SOH and Estimated R0

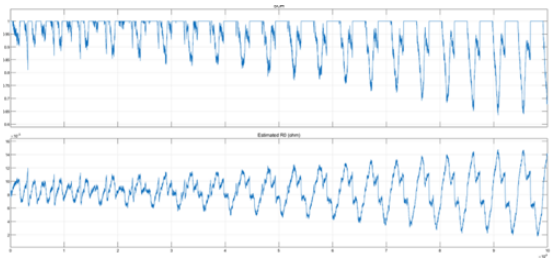

Fig. 35. SOH and Estimated R0

State of Charge & Discharge

XIV. Parallel Assembly Simulation

A. *Test the model*

First cell initial SOC = 0.1; Second cell initial SOC = 0.5;
Inside Key Components

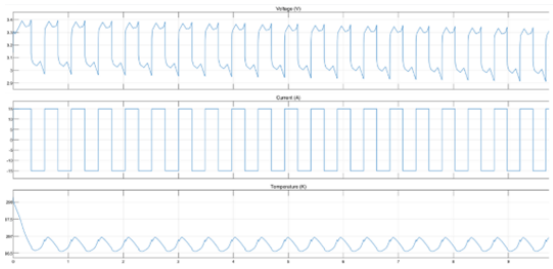

Fig. 36. State of Charge & Discharge

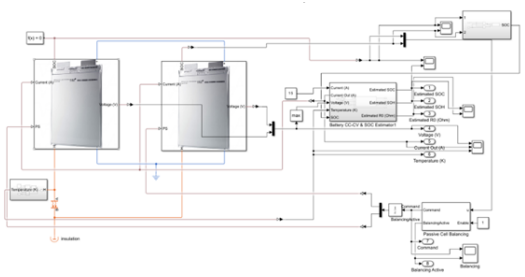

Fig. 37. Parallel Assembly Simulation

B. *Battery cc-cv & SOC Estimator*

This diagram shows a SOC Estimation System using a Battery CC-CV controller and an SOC Estimator (Kalman filter-based).

Key Components

- **Inputs**
  - **Current (A):** Current flowing through the battery.
  - **Voltage (V):** Battery voltage.
  - **Temperature (K):** Battery temperature.
  - **SOC:** Initial State of Charge.
- **Battery CC-CV:** Controls the charging process with constant current/constant voltage and outputs the SOC, Voltage, and Current Out.
- **SOC Estimator:** Uses current, voltage, and temperature to calculate the estimated SOC, the estimated SOH, and the estimated R0 (internal resistance).
- **Outputs**
  - **Estimated SOC:** State of Charge.
  - **Estimated SOH:** State of Health.
  - **Estimated R0:** Internal resistance of the battery.
  - **Current Out (A):** Output current.

This system provides real-time estimations for battery health, charge, and internal resistance using sensor data.

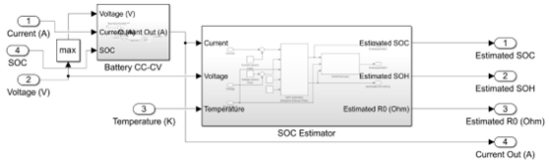

Fig. 38. Battery cc-cv & SOC Estimator

C. *Battery CC-CV*

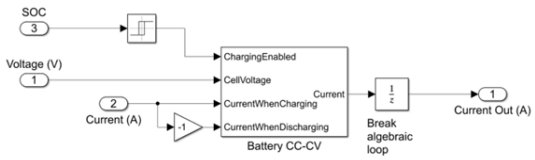

Fig. 39. Battery CC-CV

This diagram represents a **Battery CC-CV** (Constant Current-Constant Voltage) controller for battery charging and charging.

Key Components

- **SOC (State of Charge):** This input indicates the current SOC of the battery.
- **Voltage (V):** Input voltage to the controller.
- **Current (A):** Input current, differentiated for charging and discharging. The -1 multiplier inverts the current during discharge.
- **Battery CC-CV:** Manages charging and discharge currents based on SOC and voltage. Outputs different currents for charging and discharge.
- **Break Algebraic Loop:** Used to stabilize the system and ensure proper feedback flow.
- **Current Out (A):** The resultant current leaving the system.

D. *State Of Health*

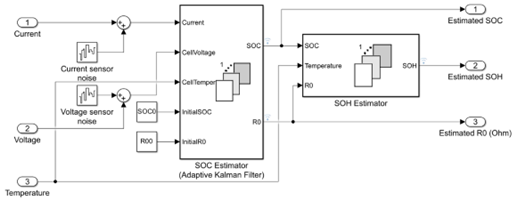

Fig. 40. State Of Health

This diagram shows an SOC Estimator using an Adaptive Kalman Filter with additional SOH Estimation for battery management.

Key Components

- **Inputs**
  - **Current (A):** The current flowing through the battery.
  - **Voltage (V):** The battery voltage.
  - **Temperature (K):** The temperature of the battery cell.
  - **SOC Estimator (Adaptive Kalman Filter):** Current sensor noise and voltage sensor noise are added to simulate real-world measurement inaccuracies.
  - **The SOC Estimator:** Uses inputs such as **current**, **voltage**, **temperature**, and **initial SOC/R0** to estimate the State of Charge (SOC). R0 is the internal resistance of the cell.

– **SOH Estimator:** The SOH Estimator uses SOC, temperature, and internal resistance (R0) to estimate the State of Health (SOH) and output the estimated internal resistance.

Outputs

- **Estimated SOC:** Estimated State of Charge.
- **Estimated SOH:** Estimated State of Health.
- **Estimated R0:** Estimated internal resistance in ohms.

This system continuously monitors and estimates the SOC, SOH, and internal resistance to ensure safe and efficient battery operation.

XV. Temperature Control

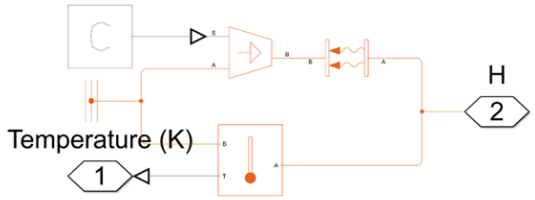

Fig. 41. Temperature Control

This diagram shows a temperature control circuit or sensor module.

Key Components

- **Temperature Input (K):** This is the input temperature signal in Kelvin (K), used as a reference for the system to monitor or regulate temperature.
- **Signal Amplification/Logic Gate:** A signal processing block compares the input signal.
- **Switch/Relay:** The block with a switch symbol indicates that it controls the flow of current or signals based on temperature thresholds or control logic.
- **Heater (H):** This output suggests that the system may activate a heating element (H) when certain conditions are met, controlled by the input temperature signal.

A. *Parallel Assembly SOC Signal Selection*

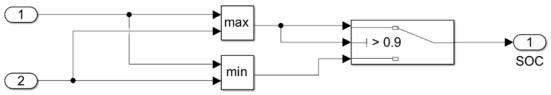

Fig. 42. Select the signal of SOC between two cells

This diagram represent a logic system that calculates or validates the State of Charge (SOC) of a battery. **Key Components**

- **Inputs (1 and 2):** These two inputs could represent different parameters or values.
- **Max/Min Functions:** These blocks compare the two input values and determine the maximum and minimum between them.
- **Threshold Logic (¿ 0.9):** This block checks if the calculated SOC exceeds 0.9 (90% SOC), possibly triggering a response if the SOC is above this level.
- **SOC Output:** The final output represents the SOC after this logic processing.

The system ensures that the SOC does not exceed a certain threshold, potentially to prevent overcharging.

B. *Cell Balancing*

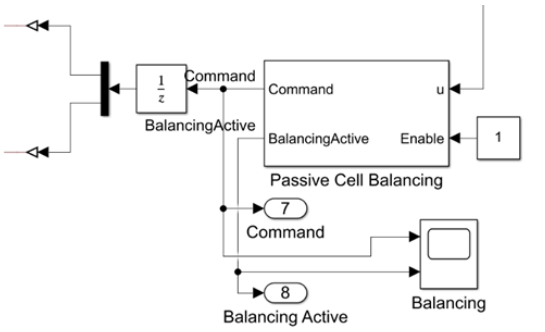

Fig. 43. Cell Balancing

This diagram represents a Passive Cell Balancing system, used in battery management to equalize the charge between cells.

Key Components

- **Balancing Active:** Indicates when the balancing process is active. This signal helps control the flow of current for balancing the cells.
- **Command Input:** The system receives a command to initiate or terminate the balancing process based on the state of the cells.
- **Passive Cell Balancing Block:** This block manages the actual balancing process by equalizing the charge between cells. The command and balancing active signals control this operation.
- **Balancing Control Logic:**
  - **Command (7):** Command signal that initiates balancing.
  - **Balancing Active (8):** Signal indicating when the balancing operation is ongoing.

This setup ensures the cells in the battery are balanced, preventing imbalances that can lead to inefficient performance or damage to the cells.

C. *Parallel Assembly Simulation Results*

D. *Parallel Assembly SOC*

Orange line: This cell started with a higher initial SOC and maintains an overall higher charge throughout the cycles. **Blue line:** The second cell started with a lower SOC but gradually catches up as both cells undergo charging and discharging cycles. cells with different initial SOCs slowly equalize over time as the system manages charge distribution between them.

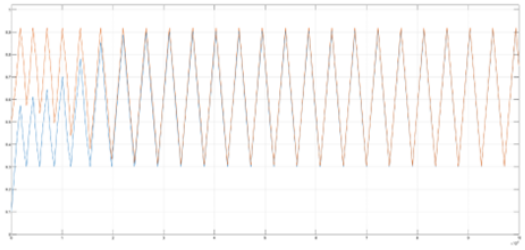

Fig. 44. Parallel Assembly SOC

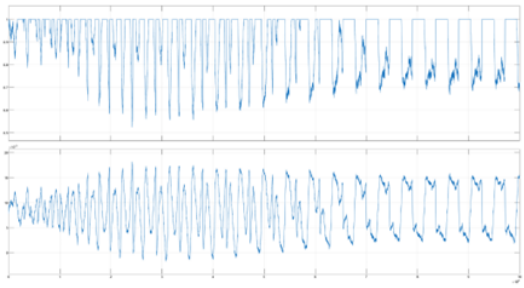

Fig. 45. Parallel Assembly SOH

E. Parallel Assembly SOH

This graph contains two plots related to the **State of Health** (SOH) of the battery cells: **Top Plot (SOH):** The SOH fluctuates between 0.5 and 1, indicating a decrease in health during periods of discharge. The sharp drops indicate stress or inefficiencies during the charge/discharge cycles, which reduces the SOH temporarily before recovering. **Bottom Plot (Estimated R0):** This shows the internal resistance (R_0) of the battery cells, which fluctuates between 5×10^{-3} and 20×10^{-3} ohms. The increasing internal resistance signifies aging or deterioration of the cells over time. The two plots together demonstrate how SOH declines and R_0 increases during cycles, indicating battery degradation.

F. Parallel Assembly Charge And Discharge

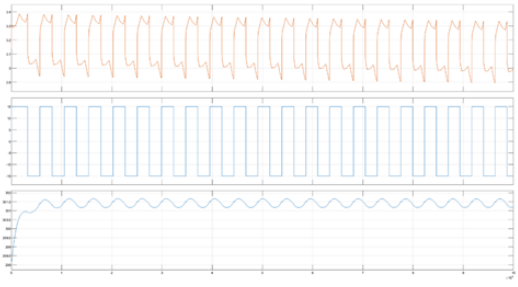

Fig. 46. Parallel Assembly Charge And Discharge

This graph shows the State of Charge and Discharge of a battery system over time. **Top Plot (Voltage):** The voltage fluctuates between 2.9V and 3.4V, showing the battery's charge and discharge cycles. **Middle Plot (Current):** The current alternates between positive (charging) and negative (discharging) with square-wave patterns, indicating regular charging and discharging cycles. **Bottom Plot (Temperature):** The temperature fluctuates slightly between 298.5K and 301K, showing some thermal variation as the battery charges and discharges. conclusion:This graph represents the regular cycling behavior of the battery with stable temperature behavior.

G. Parallel Assembly Balancing

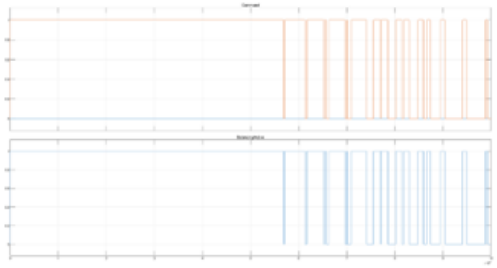

Fig. 47. Parallel Assembly Balancing

This graph illustrates the Parallel Assembly Balancing process. **Top Plot (Command):** The command signal starts at 0 and activates at about 5 units of time. The orange line shows when the command is sent to activate the balancing process, which becomes more frequent as time progresses. **Bottom Plot (Balancing Active)** The blue line represents when balancing is actively taking place. It corresponds closely to the command signal, indicating that the balancing process starts shortly after the command is issued and mirrors the command's pattern. Together, the plots indicate how the system commands and activates cell balancing over time to equalize the charge between cells.

XVI. Volt Battery Specification

For further studies the battery Pouch Cell can be implemented for real cases for simulating more complex batteries such as an EV battery pack. For further simulations the present previous model developed for the parallel assembly using the pouch cell can be used for modeling the Chevrolet Volt battery pack. Which is conformed by 192 cells in a 96S 2P configuration. For the present study case the Parallel Assembly achieved can be used for developing specific modules such as the ones integrated in the Chevrolet EV Volt model. Where the Battery pack is conformed by 7 Modules, where 4 of them correspond to a Module Assembly formed by 4 Modules of 24 cells (12 Parallel Assemblies) and 3 of them correspond to a Module Assembly formed by 3 Modules of 32 cells (16 Parallel Assemblies) conforming in total the 192 cell in the whole battery pack.

In addition, after testing the complete Battery Pack the simulation results should match the next following set of battery nominal parameters and to permit analysis of a real battery case and to optimize it according to the different

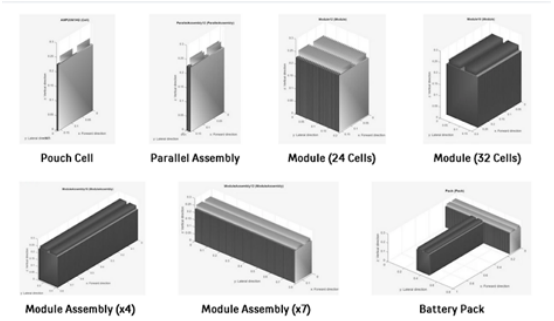

Fig. 48. Volt Battery

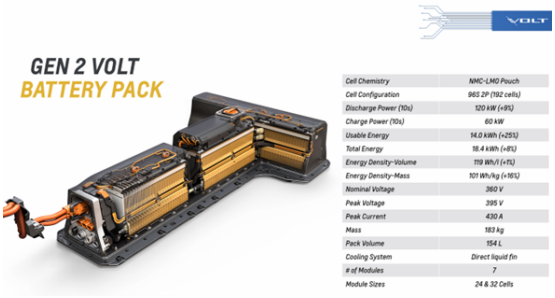

Fig. 49. Volt Battery Specifications

models to consider. In addition, the battery pack can be studied with the battery pack builder App in Matlab Simscape.

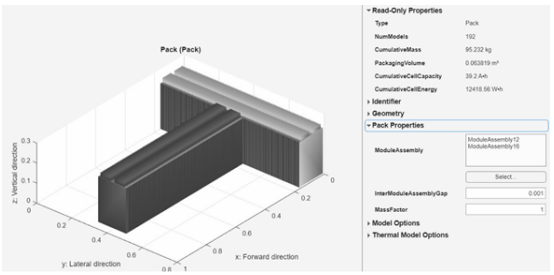

Fig. 50. Volt Battery Pack with Matlab Battery Builder

XVII. Conclusion

The conclusion for the formation process of the battery will be as follows: There is no agreed criterion for when the formation process is complete. Therefore, a chemistry independent criterion for the end of formation is needed. Gas evolution during formation is high and affects the overall process dynamics. In some cases, degassing even plays a rate-limiting role. Degassing must therefore be considered as an active part of the formation process. The effect of passive materials, i.e. separator design, and cell formats, i.e. pouch or cylindrical cells, also influence the formation process and need to be investigated. A better understanding of the relationship between the SEI/CEI structure and the performance metrics is required. Different computational methods are available at different scales, covering the most relevant aspects of formation. They should be systematically combined to optimize the process. Systematic and standardized characterisation of battery cells after formation with sufficient sample quality and size is essential to allow meaningful comparison of different formation strategies and data driven analysis. Next generation materials often increase the significance of the formation process. Thus, formation must be studied more extensively for these materials. [12].

The potential solution lies in adopting liquid electrolytes with diverse solvents and optimized dielectric and viscosity constant to enhance ion conduction rates.This necessitates a field-trial process,emphasizing the importance of consistent SEI formation, optimization studies, and the implementation of sophisticated operating emphasizing the importance of consistent SEI formation, optimization studies, and the implementation of sophisticated operating. In the context of battery separators, advanced fiber materials and post-treatment processes are critical for ensuring commercial viability. Exploring controllable nanostructures in electrospun separators,such as core-shell or hollow structures, holds promise for innovative design approaches.

References

[1] A. S. Inc., "Nanophosphate® lithium ion prismatic pouch cell amp20m1hd-a," 2011, accessed: 2024-10-10. [Online]. Available: https://liionbms.com/pdf/a123/AMP20M1HD-A.pdf

[2] ——, "A123 amp20m1hd-a nanophosphate lithium ion rechargeable cell datasheet," 2011, accessed: 2024-10-10. [Online]. Available: https://www.teklib.com/library/a123-amp20m1hd-a-design-assembly-guide/

[3] Chevrolet, "2016 chevrolet volt battery system," 2016, accessed: 2024-10-10. [Online]. Available: https://media.gm.com/content/dam/Media/microsites/product/Volt_2016/doc/VOLT_BATTERY.pdf

[4] M. Lechner, P. Mothwurf, L. Nohe, and R. Daub, "Material flow simulation in lithium-ion battery cell manufacturing as a planning tool for cost and energy optimization," *Energy Reports*, 2023, accessed: 2024-10-10. [Online]. Available: https://www.researchgate.net/publication/380187713_Material_Flow_Simulation_in_Lithium-Ion_Battery_Cell_Manufacturing_as_a_Planning_Tool_for_Cost_and_Energy_Optimization

[5] MathWorks, "Battery state-of-health estimation," 2022, accessed: 2024-10-10. [Online]. Available: https://fr.mathworks.com/help/simscape-battery/ug/battery-state-of-health-estimation.html

[6] ——, "Battery charging and discharging," 2022, accessed: 2024-10-10. [Online]. Available: https://fr.mathworks.com/help/simscape-battery/ug/battery-constant-current-constant-voltage.html

[7] ——, "Battery passive cell balancing," 2022, accessed: 2024-10-10. [Online]. Available: https://fr.mathworks.com/help/simscape-battery/ug/battery-cell-balancing.html

[8] ——, "Design and simulate battery and energy storage systems with simscape battery," 2022, accessed: 2024-10-10. [Online]. Available: https://fr.mathworks.com/videos/battery-and-energy-storage-systems-with-simscape-battery-1686604984048.html

[9] ——, "Build simple model of battery module in matlab and simscape," 2022, accessed: 2024-10-10. [Online]. Available: https://fr.mathworks.com/help/simscape-battery/ug/build-battery-module.html

[10] G. Blomgren, "The development and future of lithium ion batteries," *Journal of the Electrochemical Society*, vol. 164, p. A5019, 2016.

[11] R. Zhang *et al.*, "Balancing formation time and electrochemical performance of high energy lithium-ion batteries," *Energy*, vol. 165, pp. 108–115, 2019. [Online]. Available: https://www.sciencedirect.com/science/article/pii/S037877531830990X

[12] J. Young Cheong, "Lithium-ion battery cell formation: status and future directions towards a knowledge-based process design," *Energy & Environmental Science*, vol. 14, pp. 5000–5014, 2024.

[13] S. A. Arote, "Fundamentals and perspectives of lithium-ion batteries," *IOP Publishing Ltd.*, 2022.

[14] MathWorks, "Simscape battery essentials, part 1: Build, visualize, and simulate a battery module," 2022, accessed: 2024-10-10. [Online]. Available: https://fr.mathworks.com/videos/simscape-battery-essentials-part-1-build-visualize-and-simulate-a-battery-module-1663755729576.html

[15] ——, "Charge and discharge module assembly with coolant control," 2022, accessed: 2024-10-10. [Online]. Available: https://fr.mathworks.com/help/simscape-battery/ug/charge-discharge-module-assembly-with-coolant-control.html

[16] Y. Cheong, "Lithium-ion battery cell formation," *Energy & Environmental Science*, 2024, accessed: 2024-10-10. [Online]. Available: https://pubs.rsc.org/en/content/articlehtml/2024/ee/d3ee03559j

[17] J. Goodenough and K. Park, "The li-ion rechargeable battery: a perspective," *Journal of the American Chemical Society*, vol. 135, pp. 1167–1176, 2013.

[18] R. Schmuch, R. Wagner, G. Hörpel, T. Placke, and M. Winter, "Performance and cost of materials for lithium-based rechargeable automotive batteries," *Nature Energy*, vol. 3, pp. 267–278, 2018.

[19] D. Deng, "Li-ion batteries: basics, progress, and challenges," *Energy Science & Engineering*, vol. 3, pp. 385–418, 2015.

[20] K. Ozawa, "Lithium-ion rechargeable batteries with licoo2 and carbon electrodes: the licoo2/c system," *Solid State Ionics*, vol. 69, pp. 212–221, 1994.

[21] T. Ohzuku and R. Brodd, "An overview of positive-electrode materials for advanced lithium-ion batteries," *Journal of Power Sources*, vol. 174, pp. 449–456, 2007.

[22] M. Ue, K. Sakaushi, and K. Uosaki, "Basic knowledge in battery research bridging the gap between academia and industry," *Materials Horizons*, vol. 7, pp. 1937–1954, 2020.